EEET ECOLOGICAL ENGINEERING & ENVIRONMENTAL TECHNOLOGY

Ecological Engineering & Environmental Technology 2024, 25(7), 369–378
https://doi.org/10.12912/27197050/188713
ISSN 2719-7050, License CC-BY 4.0

Received: 2024.05.10
Accepted: 2024.05.22
Published: 2024.06.01

Utilizing Agricultural Waste for Sustainable Remediation of Textile Dyeing Effluents

Rajae Ghibate[1*], Meryem Kerrou[1], Mohammed Chrachmy[2], Meryem Ben Baaziz[2], Rachid Taouil[3], Omar Senhaji[4]

[1] Laboratory of Physical Chemistry, Materials and Environment, Faculty of Sciences and Technologies, Moulay Ismail University of Meknes, 52000, Errachidia, Morocco

[2] Laboratory of Materials Engineering for the Environment and Natural Resources, Faculty of Sciences and Technologies, Moulay Ismail University of Meknes, 52000, Errachidia, Morocco

[3] Laboratory of Mechanics, Energetics, Automation, and Sustainable Development, Faculty of Sciences and Technologies, Moulay Ismail University of Meknes, 52000, Errachidia, Morocco

[4] Laboratory of Biomolecular and Macromolecular Chemistry, Faculty of Sciences, Moulay Ismail University of Meknes, 11201, Meknes, Morocco

* Corresponding author's e-mail: rajae.ghibate@gmail.com

ABSTRACT

The primary focus of the current investigation was to assess the removal of Rhodamine B dye (RhB) from aqueous solutions using pomegranate peel as a green adsorbent. The chemical and morphological characterization of pomegranate peel was conducted through ATR-FTIR spectroscopy and SEM microscopy. The study also investigated various reactional parameters, kinetic, and adsorption isotherm in a batch system. The results revealed that RhB adsorption reaches equilibrium in about 2 hours, with an adsorption capacity of 19.41 mg/g observed at a 50 mg/L of initial RhB concentration. To model the kinetic of RhB adsorption, two well-known models (pseudo-first-order and pseudo-second-order) were applied. The pseudo-second-order model yielded a superior fit for the kinetic data, as evidenced by analyses of R^2, RMSE, ARE, and χ^2 values. Additionally, the findings suggest that the adsorption process is not solely governed by intraparticle diffusion. Furthermore, isotherm analysis revealed that the Langmuir model offered a more accurate fit to the equilibrium data, estimating the maximum removal capacity to be 47.17 mg/g. These findings suggest that pomegranate peel offers a promisingly eco-friendly and cost-effective solution for sustainable remediation of textile dyeing effluents.

Keywords: pomegranate peel, adsorption, dye removal, kinetics study, isotherm modeling.

INTRODUCTION

The textile industry is a crucial part of the global economy, providing employment opportunities and contributing to the socio-economic balance (Adane et al., 2021). However, it faces significant environmental challenges that cast doubt on its sustainability. To address these issues and ensure long-term viability, it's necessary to integrate environmental, economic, and social considerations and develop a sustainable strategy. This requires meeting environmental requirements, as the industry consumes vast amounts of water and generates wastewater with high levels of pollutants, including unfixed dyes (Periyasamy, 2024). Worldwide, the manufacturing and coloring of fabrics release around 140,000 tonnes of toxic substances annually, most of which evade conventional wastewater treatments (Guezzen et al., 2020).

Synthetic dyes are in most cases carcinogenic and toxic, causing serious harm to human health (Alsukaibi, 2022; Dutta et al., 2024). The discharge of effluents stemming from dyeing processes is frequently channeled into proximal

water bodies, encompassing agricultural fields, irrigation conduits, and other exterior aquatic reservoirs, subsequently infiltrating larger aqueous expanses such as rivers and seas (Yerima et al., 2024). Industrial effluent release from textile and dye sectors induces alterations in the physical, chemical, and biological attributes of aquatic milieus, instigating perturbations in turbidity, olfactory qualities, acoustic profiles, temperature gradients, and pH levels (Islam, Mostafa, 2018; Sudiana et al., 2022). These transformations impact community well-being, livestock welfare, wildlife populations, piscine communities, and overall biodiversity indices. The presence of dye residues within surface aquatic domains renders them aesthetically displeasing and serves as a fomite for myriad waterborne ailments (Rao and Rao, 2006; Chhandama et al., 2024). The pollution of aquatic ecosystems poses a substantial menace to public health and exerts deleterious ramifications on the overarching epidemiological and socio-economic fabric.

Rhodamine B (RhB) is one of the synthetic dyes commonly employed across diverse industries, including textiles (Al-Gheethi et al., 2022; Nyakairu et al., 2024). However, its toxicity has raised significant concerns regarding its environmental impact (Shah et al., 2024). Effluents containing RhB can pose aesthetic concerns and may have adverse effects on the environment (Nguyen et al., 2023; Umejuru et al., 2024). Research has shown that RhB can induce toxicity in aquatic organisms, particularly at concentrations exceeding 1 mg/L (Skjolding et al., 2021). To address this issue, various techniques for removing this cationic dye have been proposed and implemented (Peng et al., 2024; Vosough et al., 2024), with adsorption being one prominent method. This approach has been cited in numerous recent studies as a cost-effective, industrially feasible, promising, and efficient means of combating a spectrum of pollutants (Ghibate, Ben Baaziz, Taouil, et al., 2024; Kerrou et al., 2021), inclusive of RhB dye. In recent decades, several investigations have regarded agricultural waste as a viable source of low-cost adsorbents (Bettayeb et al., 2024; Sanad et al., 2024).

Additionally, research has demonstrated that pomegranate fruit and its extracts exhibit preventive and ameliorative properties against numerous disorders and chronic ailments (Doostkam et al., 2020; Moradnia et al., 2024). Owing to its indisputable benefits, there has been a substantial surge in demand for the fruit and its derivative products worldwide. Consequently, global production has escalated to fulfill consumer requirements, leading to a noteworthy upsurge in peel generation globally. It has been estimated that approximately 1.9 million tonnes of pomegranate peel were produced worldwide in 2017 (Ghibate et al., 2020). Thus, there arises a pressing need for its valorization. Furthermore, it is imperative to underscore that this biomass harbors significant quantities of tannins. The abundance of these phenolic compounds, characterized by hydroxyl groups, facilitates the formation of complexes with various chemical species, particularly dyes.

These considerations have prompted the exploration of a pertinent approach to ensure the sustainability of this industry, employing adsorption with pomegranate peel. This endeavor aims to serve dual ecological purposes: the valorization of agricultural waste and the remediation of effluents laden with RhB.

MATERIALS AND METHODS

Rhodamine B dye

The Rhodamine B (RhB) compound, supplied by Alfa Aesar with a purity of 98% and a molecular formula of $C_{28}H_{31}ClN_2O_3$, was used as received to prepare a stock solution. This stock solution (1000 mg/L) was diluted to the desired concentration for the adsorption experiments. Figure 1 depicts the chemical structure of RhB dye.

Pomegranate peel

Powder preparation

After being separated from the pomegranate, the peel undergoes a washing procedure with distilled water, followed by three weeks of exposure to sunlight for drying. The fragments are then crushed into a powder and subjected to several washes with distilled water until they achieve a solution devoid of coloration. The pomegranate peel powder is dried for 48 hours at 60 °C and then stored in a desiccator until needed.

Adsorbent characterization

The chemical characterization of pomegranate peel was conducted using a Bruker Alpha II Fourier Transform Infrared spectrometer, in conjunction with a diamond crystal attenuated total

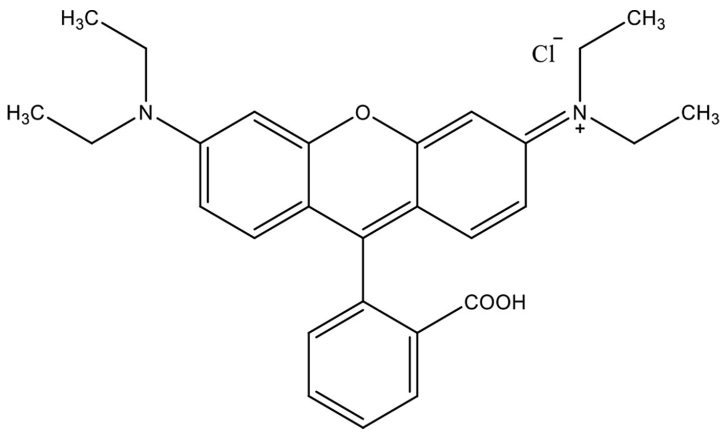

Figure 1. Chemical structure of Rhodamine B dye

reflectance accessory (ATR-FTIR). Spectral data were collected across the wavelength range of 400–4000 cm^{-1}, with a resolution set at 4 cm^{-1}. Moreover, the pomegranate peel surface morphology was scrutinized using scanning electron microscopy (SEM) with the JSM-IT500HR instrument operating at 10 kV and ambient temperature.

Batch adsorption

The experimental procedure involved the removal of RhB at its initial pH through batch adsorption. The suspension, consisting of 0.2 g of powdered pomegranate peel and 100 mL of the dye solution, was maintained under magnetic agitation at 300 rpm. The adsorption kinetic experiments were carried out over reaction times ranging from 5 to 300 minutes at 25 °C and a RhB concentration of 50 mg/L. To conduct the isotherm study, 0.2 g of pomegranate peel was immersed in 100 mL of RhB solutions with initial concentrations ranging from 50 to 650 mg/L. These suspensions were agitated for 120 minutes at 25 °C. After the experiments, the separation of the suspensions was ensured using 5 minutes of centrifugation at 3800 rpm. The residual concentrations of the supernatants were analyzed using a double-beam UV-Vis spectrophotometer at 554 nm, a characteristic wavelength of RhB dye. The quantity adsorbed per unit mass of adsorbent at time t (q_t) can be determined using the following Equation:

$$q_t = \frac{(C_0 - C_t)}{m_{ads}} \cdot V_{RhB} \quad (1)$$

where: C_0 – initial *RhB* concentration (mg/L), C_t – residual *RhB* concentration after time t of adsorption (mg/L), V_{RhB} – volume of *RhB* solution (L), m_{ads} – mass of adsorbent (g).

Kinetic study

The RhB adsorption kinetics data were analyzed using pseudo-first-order, pseudo-second-order, and intraparticle diffusion models. Below are the linear expressions of each model in the order mentioned in the text.

$$ln(q_e - q_t) = ln\, q_e - K_1 t \quad (2)$$

$$\frac{1}{q_t} = \frac{1}{K_2 q_e^2} + \frac{1}{q_e} t \quad (3)$$

$$q_t = K_{id} t^{1/2} + c \quad (4)$$

where: q_t and q_e – amounts of *RhB* adsorbed per gram of adsorbent at time t and at equilibrium, respectively (mg/g), t – contact time (min), K_1 – rate constant of the pseudo-first-order model (min^{-1}), K_2 – rate constant of the pseudo-second-order model (g/mg min), K_{id} – intraparticle diffusion rate constant ($mg/g \cdot min^{1/2}$), c – boundary layer thickness constant.

Isotherm study

The adsorption isotherm was studied using Langmuir and Freundlich models. The Langmuir isotherm model assumes structural homogeneity among all adsorption sites on the adsorbent, with adsorption limited to a monolayer. It also suggests that molecules adsorbed on adjacent sites do not interact. Consequently, further adsorption ceases at equilibrium, indicating a finite adsorption capacity. The Langmuir isotherm can be expressed as follows:

$$q_e = \frac{q_{max} K_L C_e}{1 + K_L C_e} \quad (5)$$

The subsequent equation provides the linearized form of the Langmuir model:

$$\frac{C_e}{q_e} = \frac{1}{K_L q_{max}} + \frac{C_e}{q_{max}} \quad (6)$$

where: q_{max} – adsorption capacity at its maximum (mg/g), K_L – Langmuir constant (L/mg).

The Freundlich isotherm is applied to multilayer adsorption scenarios, considering non-uniform distributions of adsorption heat and affinities across heterogeneous surfaces. The Freundlich isotherm has the following mathematical expression:

$$q_e = K_F C_e^{1/n} \quad (7)$$

The linearized expression for the Freundlich model is as follows:

$$lnq_e = lnK_F + \frac{1}{n} lnC_e \quad (8)$$

where: K_F – Freundlich coefficient linked to the adsorption capacity (mg/g)(L/g)^n, n – Freundlich's affinity coefficient (-).

Models error analysis

Error functions provide a robust way of assessing a model's suitability and underlying assumptions. Four statistical metrics were utilized (Eq. 9–Eq. 12): R^2 (coefficient of determination), ARE (average relative error), RMSE (root mean square error), and χ^2 (chi-square). A preferred model should demonstrate a coefficient of determination nearing unity while minimizing the values of ARE, RMSE, and χ^2 for enhanced accuracy and reliability.

$$R^2 = \frac{\sum_{i=1}^{N}[(q_{cal} - \bar{q}_{exp})^2]_i}{\sum_{i=1}^{N}[(q_{cal} - \bar{q}_{exp})^2]_i + \sum_{i=1}^{N}[(q_{cal} - q_{exp})^2]_i} \quad (9)$$

$$ARE = \frac{100}{N} \sum_{i=1}^{N} \left| \frac{q_{exp} - q_{cal}}{q_{exp}} \right|_i \quad (10)$$

$$RMSE = \sqrt{\frac{\sum_{i=1}^{N}[(q_{cal} - q_{exp})^2]_i}{N}} \quad (11)$$

$$\chi^2 = \sum_{i=1}^{N} \left[\frac{(q_{exp} - q_{cal})^2}{q_{cal}} \right]_i \quad (12)$$

where: q_{exp} – experimental adsorbed amount (mg/g), q_{cal} – model-predicted adsorbed amount (mg/g), N – number of data points acquired through experimentation.

RESULTS AND DISCUSSION

Adsorbent characterization

Figure 2 illustrates the infrared spectrum of pomegranate peel powder. The analysis of this spectrum depicted that the studied adsorbent possesses many oxygenated groups, including hydroxyl, carbonyl, and carboxyl. These groups facilitate the adsorption process by enabling interactions with RhB dye via hydrogen bonding, electrostatic attractions, and van der Waals forces. The frequencies corresponding to various functional groups of this biomass are displayed in Table 1.

The SEM images in Figure 3 depict pomegranate peel powder at various scales. As evident from these figures, the adsorbent surface exhibits

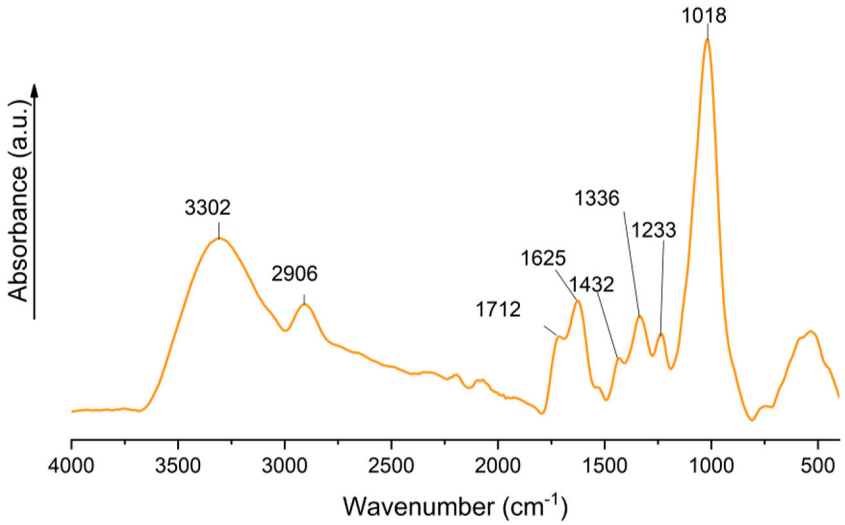

Figure 2. Infrared spectrum of the pomegranate peel powder

Table 1. Frequencies of the most important functional groups of pomegranate peel

Frequency (cm^{-1})	Assignment
3302	-OH stretching of carboxylic acid or phenol group
2906	C-H stretching vibrations of lignocellulosic components
1712	C=O stretching vibration of carboxyl group
1625	COO^- or C=C stretching vibrations of carboxylic acids
1432	C-H asymmetric deformation of methyl and methylene groups
1336	C-H symmetrical deformation of methyl group
1233	C-O stretching vibration of primary alcohol lignocellulosic components
1018	C-O stretching vibration of carboxylic acid

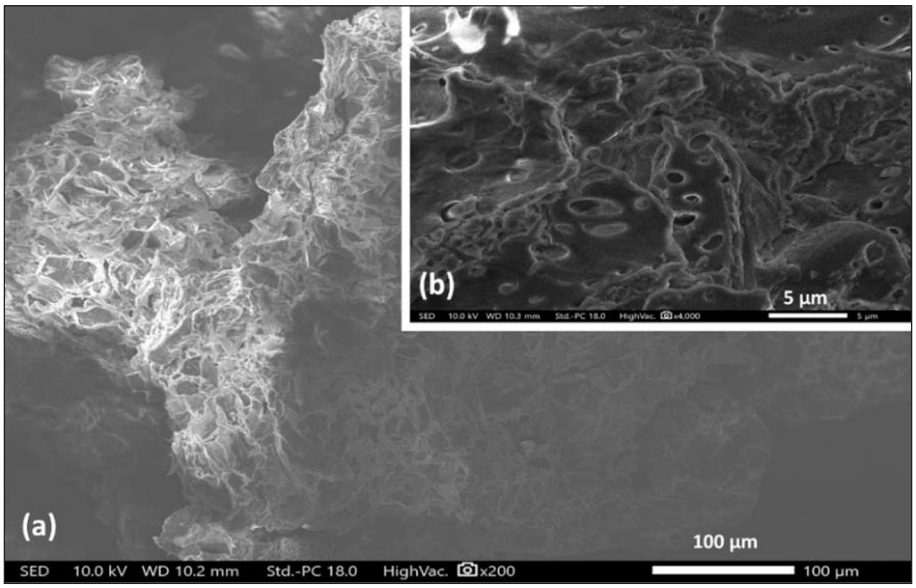

Figure 3. SEM images of pomegranate peel (a) at × 200 and (b) at × 4,000

heterogeneity. A heterogeneous surface provides more available active sites, which are conducive to the adsorption process. Furthermore, the pomegranate peel surface showcases hollow cavities and a porous structure (Figure 3b), both of which are significant in facilitating RhB adsorption.

Parameters effects

Effect of adsorption time

The RhB/pomegranate peel contact time can help ascertain the optimum time for adsorbing the dye. Additionally, the time of contact is an essential factor that governs the reaction process's kinetics and influences the adsorption's economic efficiency. As depicted in Figure 4, the quantity of RhB adsorbed initially experiences rapid growth attributable to the availability of unoccupied active sites of adsorption. Subsequently, the adsorption process decelerates due to a reduction in active adsorption sites until equilibrium is attained at 120 min. This aligns with data published by other authors (Chrachmy et al., 2024; Kooh et al., 2016). Furthermore, the equilibrium adsorption capacity for an initial RhB concentration of 50 mg/L equaled 19.41 mg/g.

Effect of initial dye concentration

The behavior of the pomegranate peel towards RhB was examined by varying its initial concentration from 50 to 650 mg/L (Figure 5). The results demonstrate that elevating the initial RhB concentration from 50 to 650 mg/L leads to a rise in adsorption capacity from 19.41 to 44.28 mg/g. Specifically, a higher RhB concentration induces a greater entrainment force attributed to the concentration gradient. Consequently, this facilitates the diffusion of RhB molecules at the interface of the pomegranate peel. Ding et al., 2014, demonstrate a

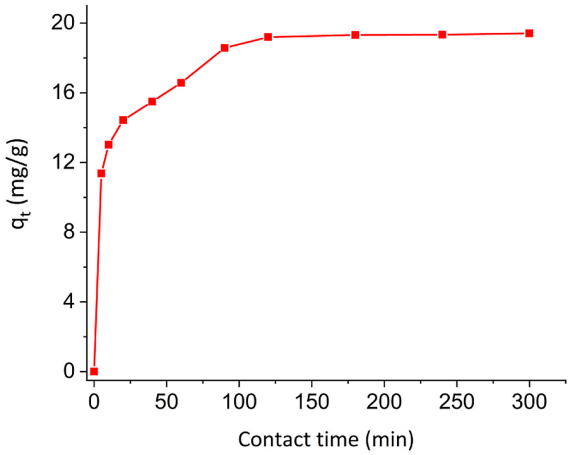

Figure 4. Effect of RhB/pomegranate peel contact time

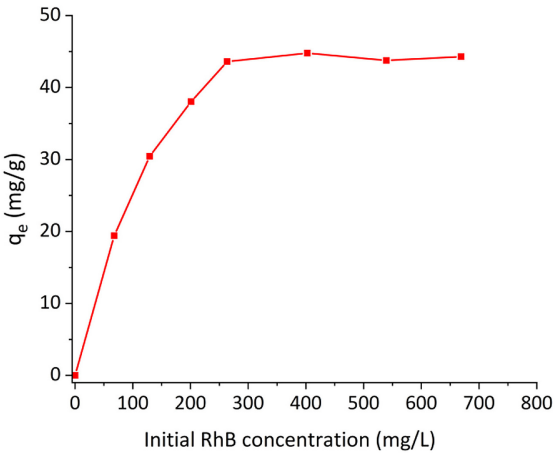

Figure 5. Effect of initial RhB concentration on adsorption effectiveness

similar behavior in their study for RhB adsorption using activated carbon derived from rice husk.

Kinetic modeling

Table 2 presents the kinetic parameters and statistical metrics for the pseudo-first-order and pseudo-second-order models. Upon reviewing Figure 6 and Table 2, it can be inferred that the pseudo-second-order model is the most appropriate for describing the adsorption of RhB onto pomegranate peel. Notably, this model has the lowest values of ARE, RMSE, and χ^2, as well as the closest coefficient of determination to one.

Figure 6c depicts the amount of RhB adsorbed over time, represented by the square root of time. The plot exhibits multilinearity, suggesting a multi-step adsorption process (Ghibate, Ben Baaziz, Amechrouq, et al., 2024; Ouallal et al., 2024). The initial sharp rise indicates the first step, likely allocated to the diffusion of RhB from the solution to the external surface of the pomegranate peel or boundary layer diffusion. Subsequently, the gradual increase represents the second stage, indicating the adsorption process's

Table 2. Adsorption kinetic parameters for RhB/pomegranate peel system

Model	Parameters at 25 °C		Statistical metrics			
Pseudo-first-order	$q_{e,cal}$ (mg/g)	K_1 (min^{-1})	R^2	ARE (%)	RMSE	χ^2
	7.53	0.0219	0.9375	71.98	11.72	443
Pseudo-second-order	$q_{e,cal}$ (mg/g)	K_2 (g/mg min)	R^2	ARE (%)	RMSE	χ^2
	19.93	0.0069	0.9993	6.10	1.27	1.67

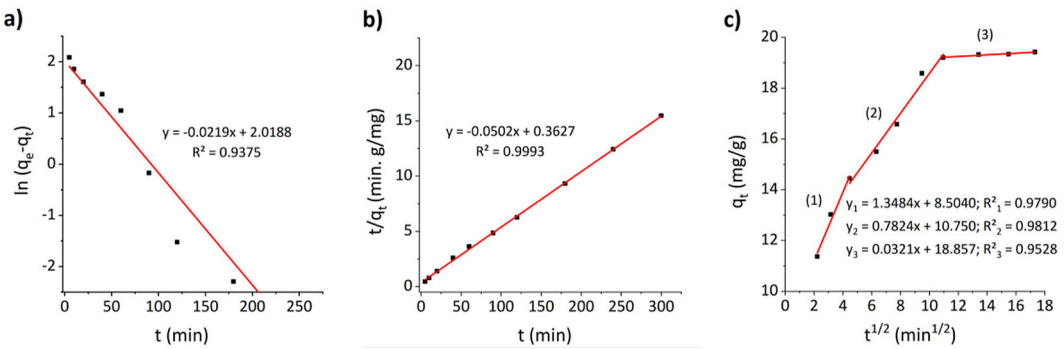

Figure 6. Analysis of RhB adsorption through pseudo-first-order (a), pseudo-second-order (b), and intraparticle diffusion (c) kinetic models

gradual progression. This stage may involve intraparticle diffusion as the limiting factor. Finally, the third stage involves further diffusion of RhB to adsorption sites. This pattern is consistent with findings of an earlier investigation (Ghibate et al., 2021), which also demonstrate similar behaviors in the adsorption of RhB by this biomass at a different concentration. The rate constant for intraparticle diffusion and the boundary layer thickness (estimated based on the slope of the second segment in Figure 6c) are reported in Table 3.

Isotherm modeling

The adsorption equilibrium of RhB on the pomegranate peel surface was investigated using Langmuir and Freundlich models at 25 °C (Figure 7). The corresponding parameters were determined and compiled in Table 4 through statistical analysis.

Figure 7 shows the graphical representations of the Langmuir and Freundlich models' linear fitting. The Langmuir model performed better than the Freundlich model in terms of fitting performance. This is supported by the R^2 value closest to one and the values of ARE, RMSE, and χ^2, which are the lowest (Table 4). These results indicate that RhB tends to form a monolayer on the pomegranate peel surface. The validation of the Langmuir model is strengthened by Figure 8. Upon a quick examination of this figure, it becomes evident that the Langmuir model is highly accurate in its predictions. Notably, the Langmuir maximum adsorption capacity (47.17 mg/g) closely aligns with the maximum experimental adsorption capacity (44.28 mg/g).

Furthermore, the dimensionless constant R_L can explain the Langmuir isotherm fundamental characteristics. This parameter is derived from the Langmuir constant (K_L) and the initial concentration (C_0), as expressed by the following equation:

$$R_L = \frac{1}{1+ K_L C_0} \tag{13}$$

The process of adsorption can be classified based on the value of the R_L criteria. When the value of R_L exceeds 1, adsorption is regarded as unfavorable. On the other hand, a value equal to 1 indicates linear adsorption behavior. An R_L value

Table 3. Kinetic parameters from the intraparticle diffusion model at 50 mg/L RhB concentration

	Step 1			Step 2			Step 3		
Parameter	$K_{id,1}$ (mg/g·min$^{1/2}$)	c_1	R^2	$K_{id,2}$ (mg/g·min$^{1/2}$)	c_2	R^2	$K_{id,3}$ (mg/g·min$^{1/2}$)	c_3	R^2
50 mg/L	1.3484	8.50	0.9790	0.7824	10.75	0.9812	0.0321	18.86	0.9528

Table 4. Equilibrium parameters for RhB adsorption

Model	Parameters at 25 °C		Statistical metrics			
Langmuir	q_{max} (mg/g)	K_L (L/g)	R^2	ARE (%)	RMSE	χ^2
	47.17	0.03	0.9973	5.73	2.17	1.09
Freundlich	n	K_F (mg/g)(L/g)n	R^2	ARE (%)	RMSE	χ^2
	3.79	9.44	0.8288	10.97	4.37	3.51

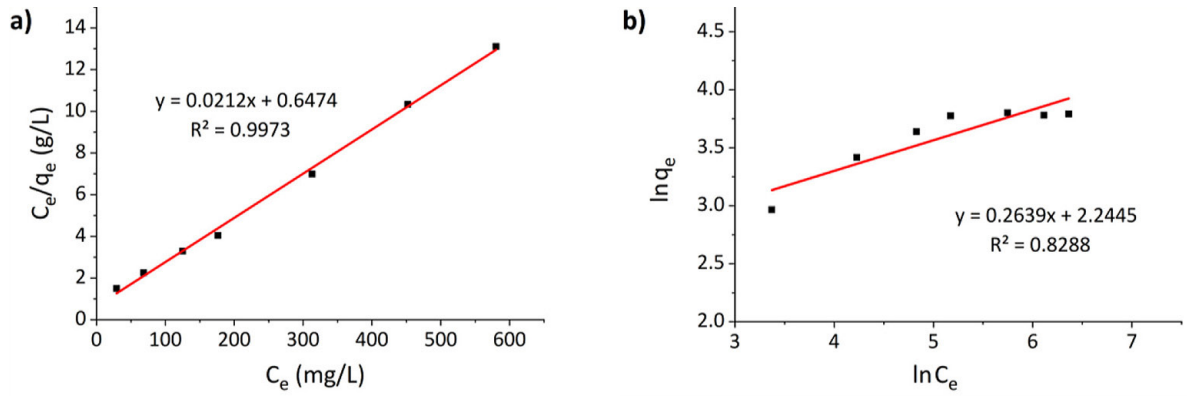

Figure 7. Modeling RhB adsorption with Langmuir (a) and Freundlich (b) linear isotherm plots

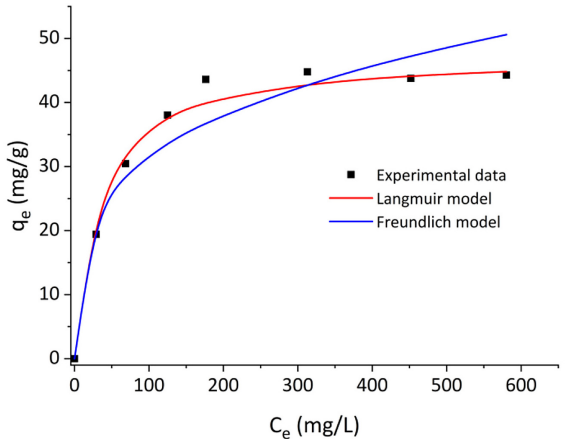

Figure 8. Experimental and predictive equilibrium data for RhB adsorption onto pomegranate peel at 25 °C

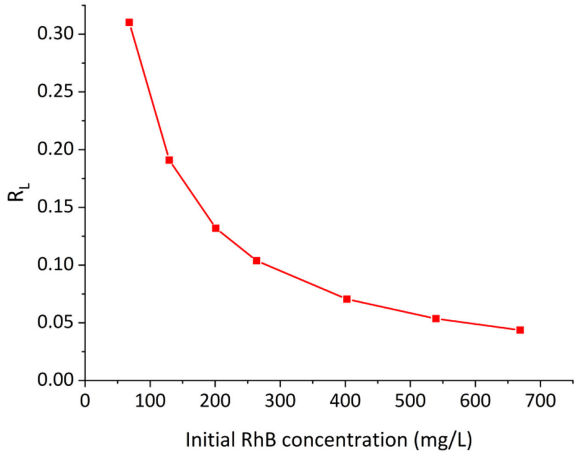

Figure 9. Plotting R_L values versus initial RhB concentrations

of zero indicates irreversible adsorption. An R_L value ranging between 0 and 1 suggests a favorable adsorption process. It can be observed from Figure 9 that the R_L values range from 0 to 1 for the entire concentration range considered. This indicates the favorability of the RhB adsorption process onto pomegranate peel.

CONCLUSIONS

Using pomegranate peel as an adsorbent for RhB has yielded promising results. The adsorption time and the initial dye concentration significantly influence RhB adsorption onto pomegranate peel. The adsorbent's chemical characterization elucidates the significant presence of oxygenated groups. These oxygenated groups likely contribute to the adsorption capacity of the pomegranate peel. The morphological characterization sheds light on the adsorbent surface's heterogeneity, providing more available active sites conducive to the adsorption process. Furthermore, the surface of the pomegranate peel showcases hollow cavities and a porous structure, both of which are significant in facilitating RhB adsorption. Statistical metrics, including R^2, ARE, RMSE, and χ^2 were utilized to assess the performance of different kinetic and isotherm models. The kinetic analysis revealed that the pseudo-second-order model outperforms the pseudo-first-order model in describing RhB adsorption. Moreover, it was observed that intraparticle diffusion does not act as the limiting step in the adsorption process. The adsorption process appears to adhere more closely to the Langmuir model, suggesting a monolayer adsorption behavior. This inference is supported by the nearly identical values of the Langmuir maximum adsorption capacity (47.17 mg/g) and the experimental maximum adsorption capacity (44.28 mg/g). Importantly, the study suggests that pomegranate peel waste can be regenerated and reused effectively as an adsorbent for removing dyes from industrial effluents, highlighting its potential for sustainable wastewater treatment solutions.

REFERENCES

1. Adane, T., Adugna, A.T., Alemayehu, E. 2021. Textile industry effluent treatment techniques. Journal of Chemistry, 2021, e5314404. https://doi.org/10.1155/2021/5314404
2. Al-Gheethi, A.A., Azhar, Q.M., Kumar, P. S., Yusuf, A.A., Al-Buriahi, A.K., Radin Mohamed, R.M.S., Al-shaibani, M.M. 2022. Sustainable approaches for removing Rhodamine B dye using agricultural waste adsorbents: A review. Chemosphere, 287, 132080. https://doi.org/10.1016/j.chemosphere.2021.132080
3. Alsukaibi, A.K.D. 2022. Various approaches for the detoxification of toxic dyes in wastewater. Processes, 10(10), 1968. https://doi.org/10.3390/pr10101968
4. Basava Rao, V.V., Rao, S.R.M. 2006. Adsorption studies on treatment of textile dyeing industrial effluent by flyash. Chemical Engineering Journal, 116(1), 77–84. https://doi.org/10.1016/j.cej.2005.09.029
5. Bettayeb, S., Merakchi, A., Lounici, H. 2024. Green almond peels a promising biosorbent for cationic dyes removal – characterization, effect of process parameters and kinetic modeling. Ecological Engineering & Environmental Technology, 25(2), 351–365.

https://doi.org/10.12912/27197050/176948

6. Chhandama, M.V.L., Chetia, A.C., Satyan, K.B., Rao, A.R., Ravishankar, G.A. 2024. Bioremediation of water polluted with dyes from textile industries using microalgae and cultivation of microalgae for multiple biorefineries. In Algae mediated bioremediation, 399–421. John Wiley & Sons, Ltd. https://doi.org/10.1002/9783527843367.ch19
7. Chrachmy, M., Ghibate, R., El Hamzaoui, N., Lechheb, M., Ouallal, H., Azrour, M. 2024. Application of raw Moroccan clay as a potential adsorbent for the removal of malachite green dye from an aqueous solution: adsorption parameters evaluation and thermodynamic study. Materials Research Proceedings, 40, 248–259. https://doi.org/10.21741/9781644903117-27
8. Ding, L., Zou, B., Gao, W., Liu, Q., Wang, Z., Guo, Y., Wang X., Liu Y. 2014. Adsorption of Rhodamine-B from aqueous solution using treated rice husk-based activated carbon. Colloids and Surfaces A: Physicochemical and Engineering Aspects, 446, 1–7. https://doi.org/10.1016/j.colsurfa.2014.01.030
9. Doostkam, A., Bassiri-Jahromi, S., Iravani, K. 2020. Punica Granatum with multiple effects in chronic diseases. International Journal of Fruit Science, 20(3), 471–494. https://doi.org/10.1080/15538362.2019.1653809
10. Dutta, S., Adhikary, S., Bhattacharya, S., Roy, D., Chatterjee, S., Chakraborty, A., Banerjee D., Ganguly A., Nanda S., Rajak, P. 2024. Contamination of textile dyes in aquatic environment: adverse impacts on aquatic ecosystem and human health, and its management using bioremediation. Journal of Environmental Management, 353, 120103. https://doi.org/10.1016/j.jenvman.2024.120103
11. Ghibate, R., Senhaji, O., Taouil, R. 2020. Valuation of pomegranate peel for cationic dye removal. International Journal of Engineering Research and Applications, 10(11), 19–22.
12. Ghibate, R., Senhaji, O., Taouil, R. 2021. Kinetic and thermodynamic approaches on Rhodamine B adsorption onto pomegranate peel. Case Studies in Chemical and Environmental Engineering, 3, 100078. https://doi.org/10.1016/j.cscee.2020.100078
13. Ghibate, R., Ben Baaziz, M., Taouil, R., Senhaji, O. 2024. Investigation of reacting parameters to improve cationic dye adsorption onto raw pomegranate peel. In J. Mabrouki & M. Azrour (Eds.), Integrated Solutions for Smart and Sustainable Environmental Conservation, 165–174. Cham: Springer Nature Switzerland. https://doi.org/10.1007/978-3-031-55787-3_12
14. Ghibate, R., Ben Baaziz, M., Amechrouq, A., Taouil, R., Senhaji, O. 2024. The performance of an eco-friendly adsorbent for methylene blue removal from aqueous solution: kinetic, isotherm, and thermodynamic approaches. Journal of the Serbian Chemical Society. https://doi.org/10.2298/JSC230317037G
15. Guezzen, B., Adjdir, M., Medjahed, B., Didi, M.A., Weidler, P.G. 2020. Kinetic study and Box–Behnken design approach to optimize the sorption process of toxic azo dye onto organo-modified bentonite. Canadian Journal of Chemistry, 98(5), 215–221. https://doi.org/10.1139/cjc-2019-0393
16. Islam, M.R., Mostafa, M.G. 2018. Textile dyeing effluents and environment concerns - a review. Journal of Environmental Science and Natural Resources, 11(1), 131–144. https://doi.org/10.3329/jesnr.v11i1-2.43380
17. Kerrou, M., Bouslamti, N., Raada, A., Elanssari, A., Mrani, D., Slimani, M.S. 2021. The use of sugarcane bagasse to remove the organic dyes from wastewater. International Journal of Analytical Chemistry, 2021, e5570806. https://doi.org/10.1155/2021/5570806
18. Kooh, M.R.R., Dahri, M.K., Lim, L.B.L. 2016. The removal of rhodamine B dye from aqueous solution using casuarina equisetifolia needles as adsorbent. Cogent Environmental Science, 2(1), 1–14. https://doi.org/10.1080/23311843.2016.1140553
19. Moradnia, M., Mohammadkhani, N., Azizi, B., Mohammadi, M., Ebrahimpour, S., Tabatabaei-Malazy, O., Mirsadeghi, S., Ale-Ebrahim, M. 2024. The power of Punica granatum: a natural remedy for oxidative stress and inflammation; a narrative review. Journal of Ethnopharmacology, 330, 118243. https://doi.org/10.1016/j.jep.2024.118243
20. Nguyen, K.M.V., Phan, A.V.N., Dang, N.T., Tran, T.Q., Duong, H.K., Nguyen, H.N., Nguyen, M. 2023. Efficiently improving the adsorption capacity of the Rhodamine B dye in a SO_3H-functionalized chromium-based metal–organic framework. Materials Advances, 4(12), 2636–2647. https://doi.org/10.1039/D3MA00123G
21. Nyakairu, G.W.A., Kapanga, P.M., Ntale, M., Lusamba, S.N., Tshimanga, R.M., Ammari, A., Shehu, Z. 2024. Synthesis, characterization and application of zeolite/Bi_2O_3 nanocomposite in removal of Rhodamine B dye from wastewater. Cleaner Water, 1, 100004. https://doi.org/10.1016/j.clwat.2024.100004
22. Ouallal, H., Chrachmy, M., El Hamzaoui, N., Lechheb, M., Ghibate, R., El-Marjaoui, H., Azrour, M. 2024. Insight on the natural Moroccan clay valorization for malachite green adsorption: kinetic and isotherm studies. Materials Research Proceedings, 40, 273–283. https://doi.org/10.21741/9781644903117-29
23. Peng, X., Xu, B., Zeng, Y., Xie, S., Zhang, Z. 2024. Waste iron oxidation reaction-assisted electrochemical flocculation for Rhodamine B extraction from wastewater: a hands-on experiment for

undergraduates. Journal of Chemical Education, 101(2), 559–566. https://doi.org/10.1021/acs.jchemed.3c00685

24. Periyasamy, A.P. 2024. Recent advances in the remediation of textile-dye-containing wastewater: prioritizing human health and sustainable wastewater treatment. Sustainability, 16(2), 495. https://doi.org/10.3390/su16020495
25. Sanad, A., Meryem, B., Badreddine, H., Chajri, F.Z., Meryeme, J., Abdellatif, A., Najoua, L., Bakasse, M., Nasrellah, H. 2024. Removal of methylene blue by low-cost adsorbent prepared from Jujube stones: kinetic and thermodynamic studies. Ecological Engineering & Environmental Technology, 25(6), 148–158. https://doi.org/10.12912/27197050/186904
26. Shah, S.F.A., Khitab, F., Rasool, S., Khattak, R., Tasmia, Gul, H., Muhammad, R., Khan, M.S., Naseem, M., Vincevica-Gaile, Z. 2024. Modified clinoptilolite for the removal of Rhodamine B dye from wastewater. Sustainability, 16(6), 2267. https://doi.org/10.3390/su16062267
27. Skjolding, L.M., Jørgensen, L.vG., Dyhr, K.S., Köppl, C.J., McKnight, U.S., Bauer-Gottwein, P., Mayer, P., Bjerg, P.L., Baun A. 2021. Assessing the aquatic toxicity and environmental safety of tracer compounds Rhodamine B and Rhodamine WT. Water Research, 197, 117109. https://doi.org/10.1016/j.watres.2021.117109
28. Sudiana, I.K., Sastrawidana, I.D.K., Sukarta, I.N. 2022. Adsorption kinetic and isotherm studies of reactive red B textile dye removal using activated coconut leaf stalk. Ecological Engineering & Environmental Technology, 23(5), 61–71. https://doi.org/10.12912/27197050/151628
29. Umejuru, E.C., Street, R., Edokpayi, J.N. 2024. The application of synthesized geopolymer for the removal of cationic dye from industrial wastewater. Results in Materials, 22, 100572. https://doi.org/10.1016/j.rinma.2024.100572
30. Vosough, M., Khayati, G.R., Sharafi, S. 2024. A novel nanocomposite for photocatalytic rhodamine B dye removal from wastewater using visible light. Environmental Research, 249, 118415. https://doi.org/10.1016/j.envres.2024.118415
31. Yerima, E.A., Ogwuche, E., Ndubueze, C.I., Muhammed, K.A., Habila, J.D. 2024. Photocatalytic degradation of acid blue 25 dye in wastewater by zinc oxide nanoparticles. Trends in Ecological and Indoor Environmental Engineering, 2(1), 50–55. https://doi.org/10.62622/TEIEE.024.2.1.50-55